EUROPEAN ORGANIZATION FOR NUCLEAR RESEARCH

TOTAL NEUTRINO AND ANTINEUTRINO CHARGED CURRENT CROSS SECTION MEASUREMENTS IN 100, 160, and 200 GeV NARROW BAND BEAMS

P. Berge[*], A. Blondel, P. Böckmann, H. Burkhardt, F. Dydak, J.G.H. De Groot, A.L. Grant, R. Hagelberg, E.W. Hughes[**], M. Krasny, H.J. Meyer, P. Palazzi, F. Ranjard, J. Rothberg[***], J. Steinberger, H. Taureg, H. Wachsmuth, H. Wahl, R. W. Williams[***], J. Wotschack and B. Wysłouch

CERN, Geneva, Switzerland

H. Blümer[+], H.D. Brummel[+], P. Buchholz[++], J. Duda, F. Eisele, B. Kampschulte, K. Kleinknecht[+], J. Knobloch[+], E. Müller[+], B. Pszola and B. Renk[+]

Institut für Physik der Universität, Dortmund, Fed. Rep. Germany[°]

R. Belusević, B. Falkenburg, M. Fiedler, R. Geiges, C. Geweniger, V. Hepp, H. Keilwerth, N. Kurz and K. Tittel

Institut für Hochenergiephysik der Universität, Heidelberg, Fed. Rep. Germany[°]

P. Debu, C. Guyot, J.P. Merlo, A. Para[+++], P. Perez, F. Perrier, J. Rander, J.P. Schuller, R. Turlay and B. Vallage

DPhPE, CEN - Saclay, France

H. Abramowicz, J. Królikowski and A. Lipniacka

Institute of Experimental Physics, University of Warsaw, Poland

[*] Visiting from Fermilab, Batavia, IL, U.S.A.
[**] Visiting from Columbia University, New York, NY, U.S.A.
[***] Visiting from University of Washington, Seattle, WA, U.S.A.
[+] Now at Universität Mainz, Fed. Rep. Germany
[++] Now at Temple University, Philadelphia, PA, U.S.A.
[+++] Now at Fermilab, Batavia, IL, U.S.A.
[°] Funded by the German Federal Minister for Research and Technology (BMFT)

ABSTRACT

Neutrino and antineutrino total charged current cross sections on iron were measured in the 100, 160, and 200 GeV narrow band beams at the CERN SPS in the energy range 10 to 200 GeV. Assuming σ/E to be constant, the values corrected for non-isoscalarity are $\sigma^{\nu}/E = (0.686 \pm 0.019) * 10^{-38}$ cm^2/(GeV $\cdot$ nucleon) and $\sigma^{\bar{\nu}}/E = (0.339 \pm 0.010) * 10^{-38}$ cm^2/(GeV $\cdot$ nucleon). Between 50 and 150 GeV no energy dependence of σ/E was observed within $\pm 3\%$ for neutrino and $\pm 4\%$ for antineutrino interactions.

1.   INTRODUCTION

In a large number of high energy neutrino experiments [1-11], total cross sections for charged current interactions of neutrinos and antineutrinos on nucleons have been measured with precisions of the order of 5-10 %. There is common agreement that the cross sections rise linearly with energy and that the antineutrino cross section is approximately half as large as the neutrino cross section. The situation concerning the absolute values is less clear (see Table 1).

The data presented in this paper come from three largely independent narrow band beam (NBB) exposures with 100, 160 and 200 GeV parent momentum using the upgraded CDHS detector. The 100 and 200 GeV data were taken in the years 1982/83, the 160 GeV data in 1984. For most of the data sets, two methods to extract the neutrino flux have been used, one based on the measurement of the parent hadron flux, the other on the measurement of the muon flux from the decay of the parent hadrons.

2.   THE NARROW BAND NEUTRINO BEAM

2.1 The Beam Layout

The general layout of the beam line is shown in Fig. 1. Protons were extracted from the CERN Super Proton Synchrotron (SPS) at 400 GeV in 1982/83 and at 450 GeV in 1984. Different extraction modes were used in order to optimize the data taking conditions for the various beam energies and polarities as shown in Table 2. The proton target was a 50 cm long beryllium rod with a diameter of 3 mm in 1982. In 1983 and 1984 it was replaced by a 50 cm long carbon target with a diameter of 30 mm.

The neutrino parents were sign selected and focused in a 117 m long beam transport system followed by a 292 m long evacuated (0.15 Torr) decay tunnel.

For the 1984 experiment the beam optics was modified to achieve a higher neutrino event rate per proton on target.   An optimum was found using a parent hadron energy of 160 GeV and operating the first group of quadrupoles differently than in the 100 and 200 GeV beams of 1982/83 [12]. As a result the momentum bite was increased to 9% compared to 6% before, and the beam divergence was increased by 40-50%.

At the end of the hadron beam line, just upstream of the decay tunnel, a movable 1.5 m long iron dump was installed (see Fig. 1). With this dump in the beam line the neutrino detector measures the neutrino flux from parents decaying upstream of the decay tunnel or passing by the beam line and creating the so-called Wide Band Beam (WBB) background. In the experiments prior to 1984 this

WBB background could only be estimated from data taken with the momentum slit (see Fig. 1) closed.

2.2 The Beam Monitors

The primary protons, the secondary hadrons, and the decay muons were monitored burst by burst. The intensity, width, and impact point of the proton beam was measured by segmented secondary emission chambers. The intensity of the hadron beam was determined with two beam current transformers (BCTs) located a few metres upstream of the decay tunnel. A movable set of segmented ionization chambers installed behind the BCTs were used to measure the position and shape of the hadron beam. The π, K, p and e composition of the beam was determined in special runs with a differential Cherenkov counter.

The different layouts of the end of the hadron beam line for the years 1982/83 and 1984 are shown in Figs. 2a and b. For the 1984 run the hadron beam monitors were rearranged and improved. The smaller upstream BCT of the 1982/83 set-up was replaced by a new one with the same design and dimensions as the second larger BCT. The electrical grounding of both BCTs was modified. They were located next to each other immediately upstream of the Cherenkov detector. The beam vacuum was extended through the two BCTs. In addition eight ionization chambers were installed around the beam pipe upstream of the BCTs to serve as beam halo monitors.

The muon flux was sampled at various radii and depths in the muon shield using solid state detectors (SSDs) and ionization chambers. Their layout was the same for the three experiments and has been described in detail earlier [13].

3. DETERMINATION OF THE NEUTRINO FLUX

The energy spectrum of neutrinos from 200 GeV parents is shown in Fig. 3.

The absolute flux of neutrinos was obtained using two largely independent methods. The first one was based on the measurement of the hadron flux with BCTs and of its composition with the Cherenkov detector. The second method employs the measurement of the muon flux with the SSDs and depends on the Cherenkov detector only for the K/π ratio but not the p/π ratio. In both methods the neutrino flux through the detector is calculated using a Monte Carlo program. This simulation includes the transport of the hadrons through the beam line, the pion and kaon decays, and - in the case of the second method - the tracking of the muons through the iron shield using recent measurements of the muon energy loss [14].

3.1 The Hadron Beam Composition

The particle ratios in the hadron beam were determined with a differential gas Cherenkov detector. Figures 4a and b show examples of pressure curves obtained in the +200 GeV and -100 GeV beam. The pion, kaon, and proton peaks are clearly visible.

In addition to the particle ratios, the Cherenkov detector provides information about other beam parameters. The divergence was determined from the width of the pion peak. The width of the proton peak measures the spread of the hadron momenta and its position determines the parent beam momentum. These results were used to adjust the hadron beam parameters in the flux simulation program.

The Cherenkov pressure gauge was calibrated by means of a refractometer to a precision of 1%. As a further test the Cherenkov detector was operated in 100, 160, and 200 GeV extracted proton beams. In all cases the measured and the nominal proton beam energies agreed within 1-2%.

The particle ratios, Table 3, are determined from the areas under the peaks of the pressure curves. The errors are of the order of 1-2% for the p/π ratios and up to 10% for the K/π ratios in the negative beams, mainly due to the uncertainty in the background estimate. The e/π ratio of 1% in the negative 160 GeV beam was determined by comparing Cherenkov curves taken with and without a 1 cm lead plate in the beam. In the 200 GeV beam electrons cannot be separated from the pion peak. Their contribution was estimated from independent particle production measurements [15] to be less than 1%. Muons from hadron decays in the beam transport system, so-called trapped muons, account for ~1% of the pion peak. Their contribution was subtracted.

In order to improve the accuracy in the measurement of the negative K/π ratios the results of reference [15] were used. They provided particle production rates for 400 GeV protons on a 500 mm beryllium target for several longitudinal and transverse momenta of the secondary particles. The K^-/π^- ratios obtained by multiplying the K^+/π^+ ratios of Table 3 by the ratios $(K^-/\pi^-)/(K^+/\pi^+)$ from ref. [15] at the mean transverse momentum accepted by the NBB line [16] were: 0.071± 0.006, 0.071 ± 0.003 and 0.054 ± 0.003 for the 100, 160 and 200 GeV beams respectively. Averaging these values with the K^-/π^- ratios of Table 3 yielded K^-/π^- = 0.071 ± 0.004, 0.069 ± 0.002 and 0.053 ± 0.003, respectively, for the three beam energies.

3.2 The Muon Flux Measurement

The muon flux was monitored by means of SSDs installed in gaps in the muon shield after ~30, 50, 70, and 90 m of iron. In each of the gaps the SSDs were arranged on rings around the beam axis plus one detector on axis. In gap 2 there were eight detectors on the 15 cm ring and four on the 30 cm ring. In all other gaps four detectors were installed on each of the 15 and 30 cm rings.

The SSDs were calibrated relative to each other with a set of movable SSDs and were found to be stable to within 1% over the whole 1982-1984 running. Their absolute response in number of muons was obtained by counting tracks in photographic emulsions exposed to a few beam pulses and separating μ from δ and cosmic ray tracks by their different angular distributions. Emulsion exposures were made in 1983 in the negative 100 and 200 GeV beams [17] and in 1984 in the negative 160 GeV beam [18]. The results from emulsion exposures in the +100 and +200 GeV beam in 1982 [19] were also used in the analysis. Typically, these emulsion calibrations have an uncertainty of 3%, dominated by track statistics and uncertainties in the size of the scanned field.

In the 100 and 200 GeV experiments the muon flux was measured using the SSDs on the 15 cm ring in gap 2 after 30 m of iron. In the 160 GeV experiment it was measured on the 30 cm ring in gap 3 after 50 m of iron.

In order to relate the observed muon flux to the flux of neutrinos through the detector the so-called trapped muons have to be subtracted. These are muons from decays of pions and kaons upstream of the decay tunnel which are "trapped" in the beam line and transported along with the hadrons. The corresponding neutrinos form part of the WBB background. In the 160 GeV beam the trapped muon correction to the observed muon flux in gap 3 at 30 cm radius was -21±1% in the positive and -19±1% in the negative beam [20]. It was measured, at the same time as the neutrino WBB background, by moving the 1.5 m long iron dump (see Fig. 2b) into the hadron beam. The muon flux distribution corrected for δ ray effects and trapped muons is shown in Fig. 5. For the 100 and 200 GeV beams the dump was not yet installed and no direct measurements were available. From a comparison of the muon fluxes in the 160 and 200 GeV beams with the momentum slit closed, the correction was estimated to be -14±2% and -12±2% for 200 GeV [20]. The correction for the 100 GeV positive and negative beams was -13±2% and -12±2%, respectively.

Beam steering uncertainties influencing the muon flux shape introduced further errors in the neutrino flux derived from the muon flux. They were determined by Monte Carlo calculations simulating observed beam variations. They resulted in an uncertainty in the neutrino flux of ±3% , ±4%, and ±0.5% in the 100, 200 and 160 GeV beams, respectively. The error due to the beam momentum uncertainty was ±1% for 1982/3 and ±2% for the 1984 beam.

The systematic uncertainties of the neutrino flux determination using muons are summarized in Table 4. It should be noted that in the determination of the ratio of positive to negative muon flux most of these uncertainties cancel. Only small acceptance differences due to different K/π ratios remain. The total uncertainty on the neutrino to antineutrino flux ratio is ≤1%.

3.3 The Hadron Flux Measurement

The total hadron flux was measured by means of BCTs installed a few metres upstream of the decay tunnel. The BCTs are toroids around the beam pipe made of high permeability alloy foils with

a pickup coil [21]. Their electrical response was calibrated with a precision of a few 10^{-3}. Possible variations with time were monitored by injecting calibration pulses between beam bursts; the observed stability was 0.3% over several months of operation.

During beam bursts the BCT response differed from its electromagnetic calibration. This was found by comparing the π^+/π^- ratio R_{BCT} as extracted from the BCTs with R_{SSD} as extracted from the muon fluxes. Since the latter is known to ±1%, any larger difference between the two must be due to additional charge induced in the BCT. The observed percentage differences $\Delta R = (R_{SSD}-R_{BCT})/R_{SSD}$ were ΔR = -9±2% and -22±2.5% in the 100 and 200 GeV beams, respectively, representing the sum of the corrections to be applied to the BCT signals in positive and negative beams.

Additional charge in the BCT can be induced by δ-ray electrons from interactions of hadrons with material upstream or air inside the BCTs, or beam halo particles hitting the BCT structure. From special runs, with a proton beam with and without vacuum in the pipe through the BCT, it was concluded that the δ-ray effect amounted to only ~2% of the signal in either polarity. In further tests it was found that, by changing the grounding conditions of the BCT, |ΔR| could be decreased. The BCT response was affected by about equal amounts but opposite in sign for both beam polarities. Based on this observation the ΔR correction in the 100 and 200 GeV beams was shared equally between negative and positive beams, 4.5±1.5% and 11±3%, where a possible asymmetric sharing is covered by the errors.

As a consequence of the above studies, the grounding of the BCTs was modified for the 1984 experiment (160 GeV) and also the beam vacuum was extended through the BCTs. After these modifications ΔR was -4.5±2% for BCT1 (the same one as used in the 100 and 200 GeV experiments) and +3±2% for BCT2. The remaining difference was beam halo dependent as shown in Fig. 6. Increasing the amount of beam halo by varying the quadrupole focusing strengths resulted in a linear dependence of ΔR, with opposite signs for BCT1 and BCT2. When extrapolated to zero halo, both BCTs measured a π^+/π^- ratio which was, within the 2% scale error of all data points, consistent with the one measured via the muon fluxes. This was supported by the fact that both BCTs had the same response to the practically halo free 160 GeV extracted proton beam.

Since in standard 160 GeV run conditions 20% more halo was recorded in negative than in positive beam, ΔR was shared in the ratio 1.2:1, i.e. for BCT1 -2.5±1.5% and +2±1.5% for negative and positive beam, respectively. The errors are mainly due to the uncertainties in particle ratios (p/π, K/π, ...). BCT1 rather than BCT2 was used for the final flux normalisation since its R values were more stable with time; those of BCT2 varied by 3% over the duration of the experiment.

All uncertainties in the neutrino flux derived from the BCT are summarized in Table 4, including those due to long term variations of the halo effect.

It should be mentioned here that the correction of the BCT signal in the 200 GeV beam of reference [3] was only 1.3% for δ-electrons and no halo correction was applied. In the analysis of those data the positive hadron flux was obtained from the negative hadron flux via the μ^+/μ^- ratio. In this case an underestimate of the BCT correction in the negative beam leads to cross sections too small for both polarities.

4. THE EVENT SAMPLES

Neutrino interactions were recorded with the upgraded CDHS detector [22], see Fig. 7. It consisted of toroidally magnetized iron plates sandwiched with planes of scintillators. The detector was grouped in 21 modules of three types: modules 1-10 with 2.5 cm, modules 11-15 with 5 cm, and modules 16-21 with 15 cm thick iron plates. The total iron thickness of each module was 50 cm for modules 1-10 and 75 cm for the others. Each module had a diameter of 3.75 m. The total mass of the detector was ~1100 tons. In between the modules triple plane drift chambers were inserted for muon tracking. The momentum of the muon was determined from the curvature of its track in the magnetic field of the detector, with an average resolution of ±9%. The average reconstruction efficiency for the muon tracks was 96±1%. The hadronic energy E_h was measured by calorimetry with a resolution of $\sigma/E_h \approx 0.58/\sqrt{E_h}$ for modules 1-10 and of $\sigma/E_h \approx 0.70/\sqrt{E_h}$ for modules 11-15 [23].

The apparatus was triggered whenever the energy deposition in three modules was larger than one third of the energy deposited by a minimum ionizing particle traversing the complete module. For muons of momenta larger than 5 GeV, the trigger efficiency was measured to be better than 99.9% using events which were selected by an independent trigger based on hadronic energy only.

In order to determine the loss of neutrino events due to dead-time, the busy signals of the detector were folded with the spill structure of the beam intensity as measured with the muon flux in the shield. The event loss varied between 5 and 25%, depending on the beam intensity and the duration of the extraction; it was measured to better than 10% of its value. The overall uncertainty in the event samples due to dead-time is ~1%.

The charged current events were selected for the analysis according to the following criteria:

- at least five drift chambers were available for muon tracking;
- the muon momentum was larger than 7 GeV for the 160 GeV and 200 GeV data;
- the muon penetrated more than 3 m of iron for the 100 GeV data;
- the vertex was less than 1.6 m from the detector axis and outside an area around the central opening for the magnet coil; this area was 40 x 40 cm^2 in modules 1-10 and 32 x 100 cm^2 in modules 11-14.

The fiducial volumes of the detector were restricted to modules 2-14 for the 100 and 200 GeV data and to modules 2-10 for the 160 GeV data. The fiducial mass was 460±5 and 280±3 tons, respectively.

Table 2 summarizes experimental conditions and event statistics for the three beam energies.

5. RESULTS

The total cross sections are obtained by dividing the measured event sample by a Monte Carlo event sample normalized to the measured neutrino flux and assuming a linearly rising cross section. The main purpose of the Monte Carlo simulation is to correct for the events lost due to the muon momentum cut-off in the data. This correction is ~25% at E_v = 30 GeV and 4-5% at the highest neutrino energies. It is insensitive to changes, within the experimentally allowed limits, in the physics input to the Monte Carlo. The uncertainty in this correction is smaller than 10% of its value and ~1% of the event sample.

Integrating over all neutrino events with E_v > 10 or 20 GeV the cross sections obtained for SSD and BCT normalisation separately are given in Table 5. The errors given here are the flux errors only. For the 100 and 200 GeV cross sections with the BCT normalisation, the neutrino flux was obtained using the antineutrino flux multiplied with the $v/\bar{v}$ flux ratio as measured by the SSDs. Within the errors both normalisations give consistent results. For the final results as given in the last column of Table 5 the flux measurements via BCT and SSDs were averaged, weighted according to their systematic uncertainties. The antineutrino to neutrino cross section ratios, which are also given in Table 5, were obtained by only using the SSDs.

In a NBB neutrinos from pion and kaon decays are separated in the energy radius space, see Fig. 8. Therefore cross sections for v_π and v_K can be determined separately. They are given in Table 6 and Fig. 9. The systematic errors quoted in Table 6 and Fig. 9 exclude a common 2% scale error which is due to uncertainties in the flux measurement (1%), the Cherenkov ratios (0.5%), the dead-time measurement (0.5%), the fiducial mass (1%), the reconstruction efficiency (0.5%), and the acceptance calculations (1%).

There is good agreement between the results obtained in the 100, 160 and 200 GeV beams. No significant deviation from a linear cross section rise with energy is visible. A straight line fit to the combined v and $\bar{v}$ data points gives a 1.5±3.0% and 0.1±4.0% rise of σ/E between 50 and 150 GeV for neutrinos and antineutrinos, respectively. The fit takes the correlation through the well measured v to $\bar{v}$ flux ratio into account. The effect of the W boson propagator was not included. It induces a σ/E variation of -0.7% over this energy range.

The energy dependence of the cross section was also determined from the 160 GeV data alone. In this case point to point errors are statistical only apart from the error in the K/π ratios. To be independent of the energy calibration of the neutrino detector, events were binned radially and the corresponding energies were determined using the energy radius relation of the NBB. The corresponding cross section values are given in Table 7. All v_π events were grouped in one bin to be independent of uncertainties in the beam divergence. A straight line fit to the data points gives an energy dependence of σ/E between 50 and 150 GeV of 0.5±4.1% for the neutrino and 2.5±6.5% for the antineutrino cross section, again consistent with no energy dependence. The errors include the uncertainties in the K/π ratios and a ±2% uncertainty in the neutrino beam momentum.

Assuming a linearly rising cross section, the final cross section slopes are obtained by averaging the results from the three beam energies weighted according to their errors. The values corrected for the neutron excess in iron (non-isoscalarity correction: -2.5% for v, +2.3% for $\bar{v}$) are:

$$\sigma^v/E = (0.686 \pm 0.002 \pm 0.019) * 10^{-38} \text{ cm}^2/(\text{GeV·nucleon})$$

$$\sigma^{\bar{v}}/E = (0.339 \pm 0.003 \pm 0.009) * 10^{-38} \text{ cm}^2/(\text{GeV·nucleon})$$

$$\sigma^{\bar{v}}/\sigma^v = 0.494 \pm 0.005 \pm 0.007.$$

The first error is statistical and the second systematic including the 2% scale error.

6.   DISCUSSION AND CONCLUSION

The measurements presented here give neutrino and antineutrino cross sections on an iron target. They come from three independent experiments in 100, 160, and 200 GeV NBBs. The neutrino fluxes were measured with two methods based on the parent hadron flux and the flux from decay muons. Both methods give consistent results. The results confirm a linear rise of neutrino and antineutrino cross sections within ±0.03 and 0.04% per GeV, respectively. The absolute cross section values agree with recent results coming from the CCFRR experiment at FNAL [10] and the revised results from the BEBC experiment at CERN [7], and are at variance with other results of comparable precision published previously [2,3,6].

The cross-sections reported here are higher than previous CDHS results [3]. The origin of this discrepancy is not precisely understood. In the meantime, however, various effects have been studied in more detail. The present measurements are therefore considered to be systematically more reliable, in particular due to the agreement of the neutrino flux determination based on both muon and hadron flux measurements, respectively.

Note that all cross sections and structure functions published by CDHS after 1979 were normalized to the cross section values of reference [3]. In order to account for the new values the cross sections in Table 2 and Fig. 7 of reference [11] should be multiplied by 1.14 for neutrinos and 1.11 for antineutrinos. The structure functions given in Tables 4 and 5 of the same paper should be scaled up by 13% and 11% respectively.

ACKNOWLEDGEMENTS

REFERENCES

1. T. Eichten et al., Phys. Lett. 46B, 274 (1973).
2. B.C. Barish et al., Phys. Rev. Lett. 39, 1595 (1977).
3. J.G.H. deGroot et al., Z.Phys.C1, 143 (1979).
4. A.E. Asratyan et al., Phys.Lett. 76B, 239 (1978).
5. D.C. Colley et al., Z.Phys.C2, 187 (1979).
6. M. Jonker at al., Phys. Lett. 99B, 265 (1981) and Phys. Lett. 100B, 520(E) (1981).
7. P. Bosetti et al., Phys. Lett. 110B, 167 (1982); updated in M. Aderholz et al., CERN/EP 86-31 (to be published in Phys.Letters B): $(\sigma/E)^V = (0.723 \pm 0.013 \pm 0.036)$ and $(\sigma/E)^V = (0.351 \pm 0.010 \pm 0.016)$, in units of $10^{-38}\,cm^2/(GeV \cdot nucleon)$.
8. N.J. Baker et al., Phys. Rev. Lett. 51, 735 (1983).
9. G.N. Taylor et al., Phys. Rev. Lett. 51, 739 (1983).
10. R. Blair et al., Phys. Rev. Lett. 51, 343 (1983).
11. H. Abramowicz et al., Z.Phys.C17, 283 (1983).
12. A. Grant and J.M. Maugain, CERN/EF/BEAM 83-2.
13. G. Cavallari et al., IEEE Trans. on Nucl. Sc., Vol. NS-25, 600 (1978); W. Venus and H. Wachsmuth, CERN-TCL-int. 73-2; E.H.M. Heijne, CERN Yellow Report, CERN 83-06.
14. W. Lohmann, R. Kopp and R. Voss, CERN Yellow Report, CERN 85-03.
15. H. Atherton et al., CERN Yellow Report, CERN 80-07.
16. H. Keilwerth, Doctoral Thesis, University of Heidelberg, 1986.
17. H. Wachsmuth, CERN/EP/NBU/86-01.
18. I. Abt and R. Jongejans, Nucl. Instrum. Methods A235, 85 (1985).
19. H. Wachsmuth and J. Wotschack, CERN/EP/NBU-85-01.
20. H. Wachsmuth and J. Wotschack, CERN/EP/NBU-86-02.
21. see e.g. K. Unser, CERN-ISR-OP/81-14.
22. M. Holder et al., Nucl. Instrum. Methods 148 (1978) 235; H. Abramowicz et al., Phys. Rev. Lett. 17 (1986) 298.
23. H. Abramowicz et al., Nucl. Instrum. Methods 180 (1981) 429.

<u>Table 1</u>

Previous cross section measurements. Where two errors are given
the first is statistical, the second systematic.

EXPERIMENT	E_ν(GeV)	σ^ν/E (10^{-38} cm^2/GeV)	$\sigma^{\bar\nu}/E$ (10^{-38} cm^2/GeV)	Ref.
GGM*)	1 - 10	0.74 $\pm$ 0.02 $\pm$ 0.07	0.28 $\pm$ 0.01 $\pm$ 0.03	[1]
CITFR	45 - 205	0.609 $\pm$ 0.030 $\pm$ 0.025	0.290 $\pm$ 0.015 $\pm$ 0.012	[2]
CDHS*)	30 - 190	0.62 $\pm$ 0.03	0.30 $\pm$ 0.02	[3]
ITEP-IHEP	3 - 30	0.72 $\pm$ 0.07	0.32 $\pm$ 0.03	[4]
BEBC	10 - 50	0.73 $\pm$ .08	0.32 $\pm$ 0.06	[5]
CHARM	20 - 200	0.604 $\pm$ 0.032	0.301 $\pm$ 0.018	[6]
BEBC	20 - 200	0.657 $\pm$ 0.012 $\pm$ 0.027	0.309 $\pm$ 0.009 $\pm$ 0.013	[7]
FNAL-15'	10 - 240	0.62 $\pm$ 0.05		[8]
FNAL-15'	5 - 250		0.340 $\pm$ 0.019 $\pm$ 0.022	[9]
CCFRR	30 - 240	0.669 $\pm$ 0.003 $\pm$ 0.024	0.340 $\pm$ 0.003 $\pm$ 0.020	[10]

*) Not corrected for non-isoscalarity

Table 2

Run conditions and event statistics

year	1982/83				1984	
E_{proton}(GeV)	400				450	
E_{beam} (GeV)	100		200		160	
Extraction mode	1000 μs / (1-5) • 23 μs				300 μs	
Polarity	ν	$\bar{\nu}$	ν	$\bar{\nu}$	ν	$\bar{\nu}$
Protons on tgt. (10^{18})	0.21	0.48	0.48	0.42	5.50	0.60
Events after cuts	10,000	9,000	11,000	2,500	200,000	9,000

Table 3

Particle ratios as determined with the Cherenkov detector

		BEAM ENERGY (GeV)		
		100	160	200
pos.	p/π	0.587 ± 0.020	1.546 ± 0.025	4.260 ± 0.090
	K/π	0.092 ± 0.006	0.132 ± 0.003	0.154 ± 0.007
	e /π	0.027 ± 0.005	0.005 ± 0.003	0.0
neg.	p/π	<0.025	0.010 ± 0.005	<0.01
	K/π*)	0.072 ± 0.005	0.065 ± 0.004	0.050 ± 0.006
	e /π	0.058 ± 0.011	0.010 ± 0.005	0.0
*) Used (see text):		0.071 ± 0.004	0.069 ± 0.002	0.053 ± 0.003

Table 4

Systematic uncertainties on the neutrino flux [%]

METHOD	BCT			SSD		
E_{beam} (GeV)	100 / 200		160	100 / 200		160
Absolute calibration	1	1	1	3.5	3.5	2.8
Halo correction	2.5	2.8	1.5	-	-	-
Trapped muon corr.	-		-	2	2	1
Beam steering	-		-	3	4	0.5
Beam momentum	-		-	1	1	2
Particle ratios, pos.	2.2	2.2	2.2	-		-
neg.	1	1	1	-		-
TOTAL positive	3.5	3.7	3.0	5.1	5.8	3.6
negative	2.9	3.1	2.1	5.1	5.8	3.6

Table 5

Cross sections σ/E on iron from the 100, 160 and 200 GeV data separately for BCT and SSD flux normalisations. The errors are the flux errors only. In the last column, BCT and SSD flux measurements are averaged; here and in the cross section ratios the first error is statistical, the second the complete systematic error.

	E_{beam} (GeV)	E_ν (GeV)	$<E_\nu>$ (GeV)	BCT (10^{-38} cm^2/GeV)	SSD (10^{-38} cm^2/GeV)	Average (10^{-38}cm^2/GeV)
	+100	10 - 100	50	0.680 ± 0.023	0.711 ± 0.036	$0.691 \pm 0.007 \pm 0.027$
ν	+160	20 - 160	85	0.710 ± 0.020	0.703 ± 0.025	$0.707 \pm 0.002 \pm 0.022$
	+200	20 - 200	112	0.689 ± 0.025	0.746 ± 0.042	$0.708 \pm 0.007 \pm 0.029$
	-100	10 - 100	47	0.326 ± 0.009	0.339 ± 0.017	$0.332 \pm 0.004 \pm 0.012$
$\bar{\nu}$	-160	20 - 160	72	0.332 ± 0.006	0.335 ± 0.012	$0.333 \pm 0.004 \pm 0.009$
	-200	20 - 200	87	0.317 ± 0.009	0.346 ± 0.020	$0.325 \pm 0.007 \pm 0.012$
	100	10 - 100			$0.477 \pm 0.008 \pm 0.007$	
$\bar{\nu}/\nu$	160	20 - 160			$0.477 \pm 0.006 \pm 0.007$	
	200	20 - 200			$0.464 \pm 0.011 \pm 0.007$	

Table 6

Average cross section slopes for neutrinos from pion and kaon decays.
The first error is statistical, the second systematic, excluding the common 2% scale error.

	E_{beam} (GeV)	$<E_\nu>$ (GeV)	σ^ν/E (10^{-38} cm^2/GeV)	$\sigma^{\bar\nu}/E$ (10^{-38} cm^2/GeV)	$\sigma^{\bar\nu}/\sigma^\nu$
	100	31	0.682±0.008±0.020	0.327±0.004±0.008	0.479±0.008±0.008
ν_π	160	50	0.706±0.002±0.018	0.332±0.005±0.007	0.470±0.007±0.008
	200	61	0.707±0.009±0.023	0.338±0.009±0.010	0.478±0.014±0.008
	100	83	0.724±0.012±0.051	0.346±0.007±0.022	0.478±0.013±0.042
ν_K	160	121	0.708±0.003±0.023	0.337±0.008±0.012	0.476±0.012±0.019
	200	143	0.711±0.010±0.040	0.306±0.015±0.020	0.430±0.022±0.032
Average:			0.703±0.002±0.019	0.331±0.003±0.009	0.471±0.005±0.007

Table 7

Total cross sections from the 160 GeV data as function of neutrino energy.
The data point at 50 GeV is averaged over all neutrinos from pion decay. The other data points
correspond to neutrinos from kaon decay in radial bins around the beam axis.
The errors are statistical only.

	Radius (cm)	$<E_\nu>$ (GeV)	σ^ν/E (10^{-38} cm^2/GeV)	$\sigma^{\bar{\nu}}/E$ (10^{-38} cm^2/GeV)
ν_π	0 - 100	50	0.706 ± 0.002	0.331 ± 0.005
ν_K	157 - 206	82	0.700 ± 0.014	0.335 ± 0.030
	117 - 157	101	0.708 ± 0.008	0.336 ± 0.016
	77 - 117	121	0.710 ± 0.007	0.337 ± 0.012
	0 - 77	145	0.711 ± 0.007	0.341 ± 0.012

FIGURE CAPTIONS

Fig. 1   Layout of the CERN SPS neutrino facility.

Fig. 2   Layout of the end of the hadron beam line for a) the 100 and 200 GeV experiment in 1982/83, and b) the 160 GeV experiment in 1984.

Fig. 3   Neutrino energy spectrum for the 200 GeV neutrino beam averaged over the area of the detector.

Fig. 4   Cherenkov pressure curves a) for the 200 GeV positive, and b) for the 100 GeV negative hadron beam.

Fig. 5   Radial muon flux distributions in the 160 GeV beam for a) positive and b) negative beam polarity. The data in gaps 2, 3, 4, corresponding to 40, 76, 116 GeV minimum muon momentum, are averages over the SSDs on the same radius and are corrected for the trapped muon flux. The Monte Carlo calculations are normalized to the data points in gap 3 at R=30 cm. The average momentum of the parent pions and kaons is 158 GeV.

Fig. 6   The π^+/π^- ratio as measured via BCT1 and BCT2 as a function of beam halo in the 160 GeV beam. When extrapolated to zero halo, both BCTs measure a π^+/π^- ratio which is, within the 2% scale error of all data points, consistent with the one measured via the muon fluxes (SSDs). The difference between the π^+/π^- ratios as measured via BCTs and SSDs is the ΔR referred to in the text.

Fig. 7   The upgraded CDHS detector.

Fig. 8   Neutrino data from the 160 GeV beam as a function of measured energy $E_\nu = E_{had} + p_\mu$ and radial distance from the beam axis.

Fig. 9   Average ν_π and ν_K cross sections from the 100, 160 and 200 GeV data. The statistical and systematic errors were added in quadrature, excluding an overall 2% scale error common to all data points.

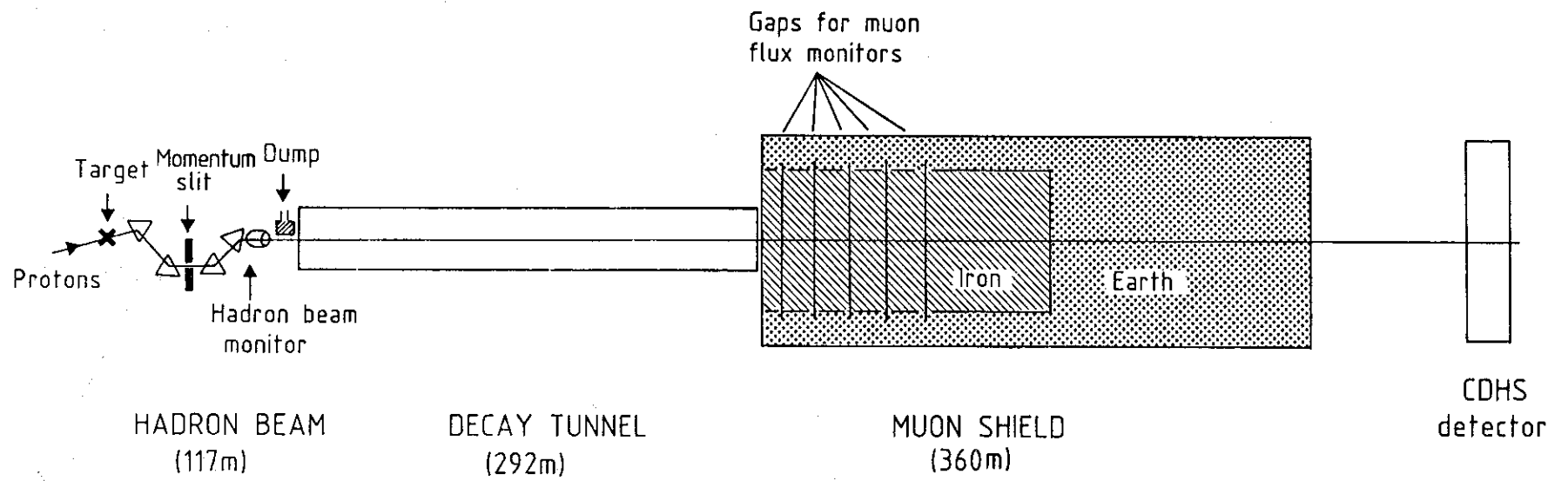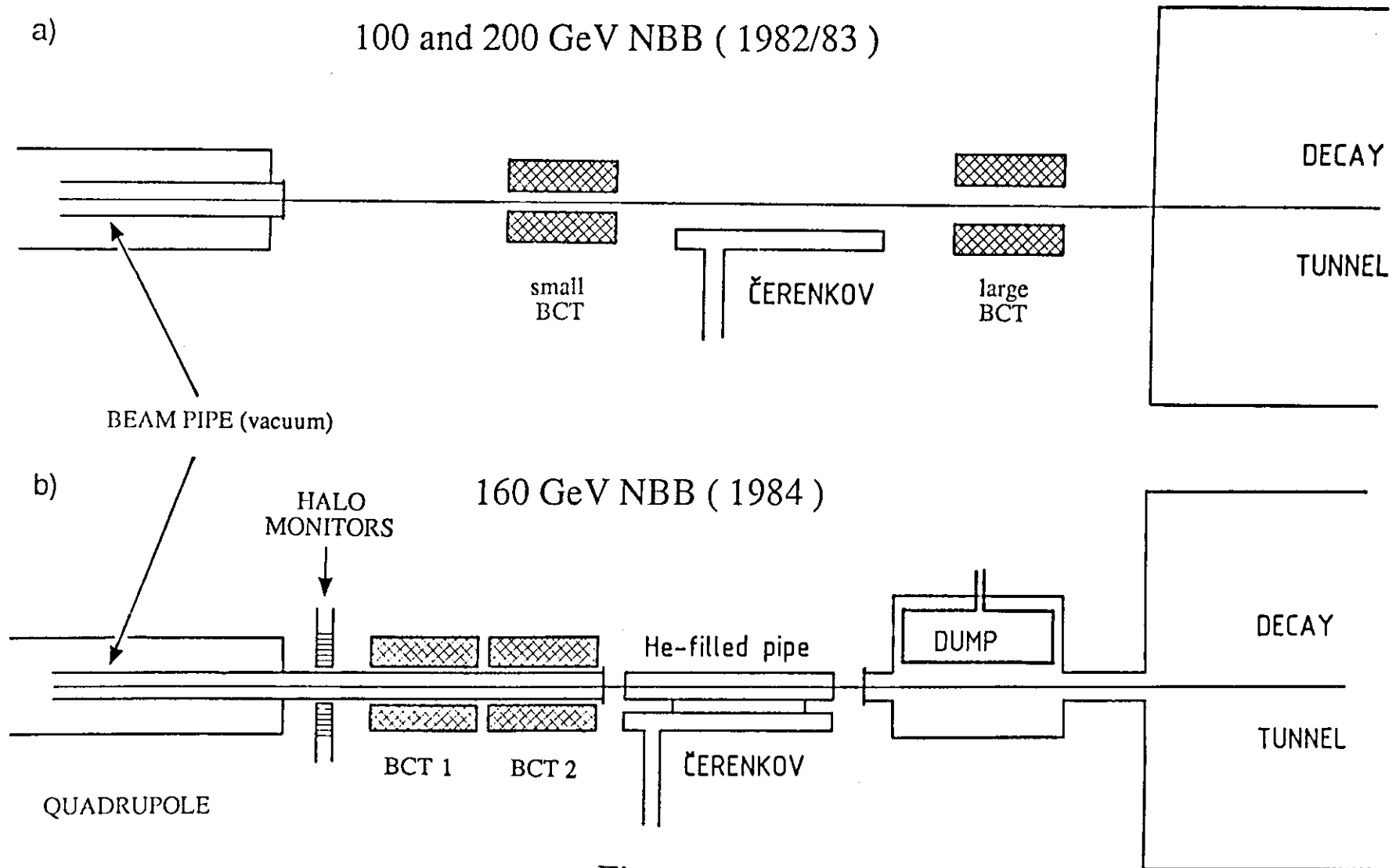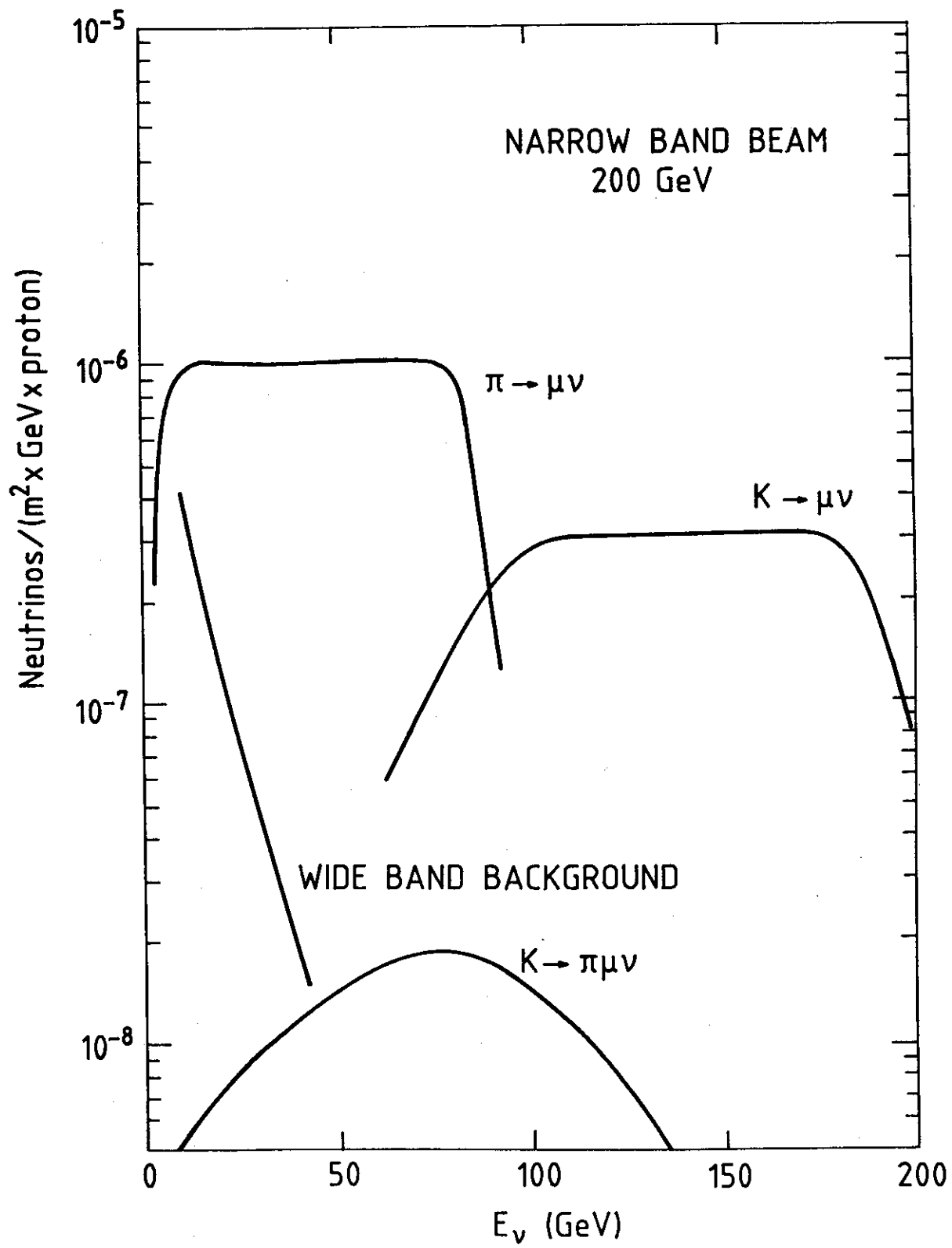Fig. 10   Cross sections from the 160 GeV data as a function of energy. Errors are statistical only.

Gaps for muon
flux monitors

Target
Momentum
slit
Dump

Protons

Hadron beam
monitor

Iron

Earth

CDHS
detector

HADRON BEAM
(117m)

DECAY TUNNEL
(292m)

MUON SHIELD
(360m)

Fig. 1

a) 100 and 200 GeV NBB (1982/83)

DECAY

TUNNEL

small
BCT

ČERENKOV

large
BCT

BEAM PIPE (vacuum)

b) 160 GeV NBB (1984)

HALO
MONITORS

He-filled pipe

DUMP

DECAY

TUNNEL

BCT 1   BCT 2

ČERENKOV

QUADRUPOLE

Fig. 2

NARROW BAND BEAM
200 GeV

$\pi \rightarrow \mu \nu$

$K \rightarrow \mu \nu$

10^{-5}

10^{-6}

10^{-7}

10^{-8}

Neutrinos/(m^{2}x GeV x proton)

WIDE BAND BACKGROUND

$K \rightarrow \pi \mu \nu$

0   50   100   150   200

E_ν (GeV)

Fig. 3

Fig. 4

●■▲ Data in gap 2, 3, 4
—— Monte Carlo calculation

Fig. 5

Fig. 6

Fig. 7

Fig. 8

1.0

0.9

● 100 GeV NBB 1982/83

0.8

■ 160 GeV NBB 1984

▲ 200 GeV NBB 1982/83

$\sigma/E \times 10^{-38}$ cm^2/(nucleon · GeV)

0.7

0.6

ν_π

ν_k

0.5

0.4

0.3

$\overline{\nu}_\pi$

$\overline{\nu}_k$

0.2

0.1

0

50

100

150

E_ν (GeV)

Fig. 9

Fig. 10